Titania Mixed with Silica: A Low Thermal-Noise Coating Material for Gravitational-Wave Detectors

Graeme I. McGhee,[1] Viola Spagnuolo,[2,3] Nicholas Demos,[4] Simon C. Tait,[1] Peter G. Murray,[1] Martin Chicoine,[5] Paul Dabadie,[6] Slawek Gras,[4] Jim Hough,[1] Guido Alex Iandolo,[2,3] Ross Johnston,[1] Valérie Martinez,[6] Oli Patane,[7] Sheila Rowan,[1] François Schiettekatte,[5] Joshua R. Smith,[8] Lukas Terkowski,[9] Liyuan Zhang,[10] Matthew Evans,[4] Iain W. Martin,[1] and Jessica Steinlechner[1,2,3,*]

[1]*SUPA, School of Physics and Astronomy, University of Glasgow, Glasgow G12 8QQ, Scotland*
[2]*Maastricht University, Minderbroedersberg 4-6, 6211 LK Maastricht, The Netherlands*
[3]*Nikhef, Science Park 105, 1098 XG Amsterdam, The Netherlands*
[4]*Massachusetts Institute of Technology, 185 Albany Street, Cambridge, Massachusetts 02139, USA*
[5]*Département de Physique, Université de Montréal, Montréal, Québec, Canada,*
[6]*Université de Lyon, Université Claude Bernard Lyon 1, CNRS, Institut Lumière Matière, F-69622 Villeurbanne, France*
[7]*Department of Physics, California State University Fullerton, Fullerton, California 92831, USA*
[8]*Nicholas and Lee Begovich Center for Gravitational-Wave Physics and Astronomy, California State University, Fullerton, Fullerton, California 92831, USA*
[9]*Institut für Laserphysik und Zentrum für Optische Quantentechnologien, Universität Hamburg, Luruper Chaussee 149, D-22761 Hamburg, Germany*
[10]*LIGO Laboratory, California Institute of Technology, Pasadena, California 91125, USA*

(Received 20 July 2023; accepted 15 September 2023; published 23 October 2023)

Coating thermal noise is one of the dominant noise sources in current gravitational wave detectors and ultimately limits their ability to observe weaker or more distant astronomical sources. This Letter presents investigations of TiO_2 mixed with SiO_2 (TiO_2:SiO_2) as a coating material. We find that, after heat treatment for 100 h at 850 °C, thermal noise of a highly reflective coating comprising of TiO_2:SiO_2 and SiO_2 reduces to 76% of the current levels in the Advanced LIGO and Advanced Virgo detectors—with potential for reaching 45%, if we assume the mechanical loss of state-of-the-art SiO_2 layers. Furthermore, those coatings show low optical absorption of <1 ppm and optical scattering of $\lesssim 5$ ppm. Notably, we still observe excellent optical and thermal noise performance following crystallization in the coatings. These results show the potential to meet the parameters required for the next upgrades of the Advanced LIGO and Advanced Virgo detectors.

DOI: 10.1103/PhysRevLett.131.171401

Introduction.—Gravitational waves are generated by massive, accelerating objects such as merging black holes and neutron stars. These waves, predicted by Einstein more than 100 years ago, cause transverse quadrupole strains in space resulting in dimension changes in appropriately oriented objects [1,2].

To measure these length changes, enhanced Michelson interferometers have been developed to monitor the distance between highly reflective (HR) mirrors suspended several kilometers apart. Since the first detection in 2015, a large number of gravitational-wave signals have been observed [3–6] by the Advanced LIGO (aLIGO) [7] and Advanced Virgo (AdV) [8] detectors. One of the major limitations to the detectors' sensitivity is displacement noise of the mirrors' surfaces arising from Brownian thermal motion in the mirror coatings. The magnitude of the coating thermal noise (CTN) amplitude spectral density is given by [9]

$$x(f) = \sqrt{\frac{2k_B T}{\pi^2 f}\frac{1}{w^2}\frac{1-\sigma_{\mathrm{sub}}-2\sigma_{\mathrm{sub}}^2}{Y_{\mathrm{sub}}}\sum_j b_j d_j \phi_j}. \quad (1)$$

Here k_B is the Boltzmann constant, T the mirror temperature, f the frequency, w the radius of the laser beam on the coating, and Y_{sub} and σ_{sub} are the Young's modulus and the Poisson ratio of the mirror substrate. d_j and ϕ_j are the thickness and the mechanical loss of the jth layer in the coating, and b_j is a weighting factor for the jth layer defined in [9]. We assume here that the mechanical losses associated with bulk motion and shear motion [10] are approximately equal ($\phi_{\mathrm{bulk}} \approx \phi_{\mathrm{shear}} \approx \phi$).

A reduction in CTN is critical to reach the required sensitivity and full astronomical potential of planned detector upgrades and future detectors. For current detectors, operating at room temperature and with a given beam size, a reduction in thickness via the use of materials with a higher contrast in refractive index, n, or a reduction in coating mechanical loss is therefore required.

The coatings of the aLIGO and AdV detectors, produced by LMA [11] via ion beam sputtering, are stacks of alternating layers of SiO_2 (low n), and Ta_2O_5 mixed with 25% TiO_2 (high n, referred to as $TiO_2:Ta_2O_5$) [12]. The optical absorption of these HR coatings is as low as ≈ 0.25 ppm at the detector wavelength of $\lambda = 1064$ nm [13]. The $TiO_2:Ta_2O_5$ layers dominate the overall mechanical loss, and therefore the CTN [14–16].

To reduce CTN, materials to replace $TiO_2:Ta_2O_5$ are being investigated [17]. Strong candidates include silicon nitride [18] and $TiO_2:GeO_2$ [19]. A current drawback of silicon nitride is the relatively high optical absorption [18]. For $TiO_2:GeO_2$, mechanical loss measurements have shown the potential for 50% CTN reduction [19], however, direct CTN measurements confirming this reduction are awaited. The absorption for an HR coating was shown to be a few ppm and recent progress with mitigating initial delamination issues due to heat treatment [20] has been made.

In this Letter, we present an extensive study of another previously identified candidate high-index material: SiO_2 mixed with TiO_2 ($TiO_2:SiO_2$) [21,22]. To investigate the effect of composition on the refractive index and mechanical loss, single layers of different compositions were produced. Two HR multilayer stacks, using SiO_2 for the low-index layers, were also studied. Investigations into the effect of heat treatment on the optical properties were carried out, and we present a comparison of mechanical loss measurements and direct CTN measurements. We discuss defect formation during heat treatment, and the onset of crystallization which, perhaps surprisingly, does not cause significant deterioration in the optical or thermal noise performance.

Coating deposition and composition.—The $TiO_2:SiO_2$ coatings were deposited by FiveNine Optics [23] using ion beam sputtering with Ti and SiO_2 targets and argon as the sputtering ion. To investigate the effects of the composition, four single layer coatings were deposited, of which three were different in composition, while that with the highest TiO_2 concentration was deposited twice, allowing consistency checks of the deposition process.

Rutherford backscattering spectrometry (RBS) was used to determine the composition of the single layers [24]. Simulations with the ion beam analysis software SIMNRA [25], using a uniform and stoichiometric layer model, allowed the measured cation ratios $Ti/(Ti + Si)$ to be estimated (see Table I). As-deposited layers contain 0.5% Ar.

TABLE I. Nominal and measured Ti-cation concentrations, n at 1064 nm at selected heat-treatment temperatures T, t, and ρ of the single layers, and t_{HR} required for $R \geq 99.9994\%$ (using $n_{SiO_2} = 1.45$). Coatings measured in their as-deposited state, with no additional heat treatment, as indicated by "none" in the T column.

Ti concentration [%]						
Target	Measured	t [nm]	T [°C]	n	t_{HR} [μm]	ρ [kg/m^3]
Single layers						
40	46.2 ± 0.4	298	none	1.77	10.83	2686 ± 50
			450	1.75	11.56	
50	58.5 ± 0.5	274	none	1.88	7.94	2889 ± 50
			450	1.86	8.63	
			750	1.88	7.94	
60	62.3 ± 0.5	272	none	1.93	7.21	2967 ± 50
			450	1.92	7.54	
			500	1.91	7.56	
60	62.6 ± 0.5	256	none	1.93	7.21	3022 ± 50
			450	1.91	7.56	
HR coatings						
50	63.2 ± 2.0		none	1.93	7.21	
60	69.5 ± 1.7		none	1.97	6.83	

Two HR multilayer stacks were also deposited, using SiO_2 as the low-n partner to the high-n $TiO_2:SiO_2$ layers—one with 63.2% Ti concentration (target 50%), using 17.5 layer pairs (starting and ending with the high-n material), and the other with a 69.5% Ti concentration (target 60%), using 21.5 layer pairs. Each layer was nominally $\lambda/4n$ in thickness to give high reflectivity. The Ti cation concentrations were verified using elastic recoil detection time of flight measurements [26] probing the elemental composition of the top four layers of each stack.

From transmission spectra of the single layers, thickness t and n were obtained using the software tool SCOUT [27]. Table I shows the results for the as-deposited single layers and for selected annealing temperatures, showing that n increases with the Ti cation concentration. For the 69.5% layers, n was estimated from a linear extrapolation of the single layers indices.

Table I also shows the calculated thickness t_{HR} of an HR stack of reflectivity $R \geq 99.9994\%$ using $TiO_2:SiO_2$ layers partnered with SiO_2. The lowest Ti concentration from the single layers would require a very thick HR coating due to the low n, as each $TiO_2:SiO_2$ layer becomes thicker, and more pairs of layers are required to generate the desired reflectivity [28,29].

Mechanical loss.—The mechanical loss of the coatings was measured using the gentle nodal support (GeNS) technique [30], in which a disk is balanced on a spherical lens. The loss is calculated from the time dependence of the amplitude decay of excited vibrational modes, measured via an optical lever readout. Comparison of the loss before

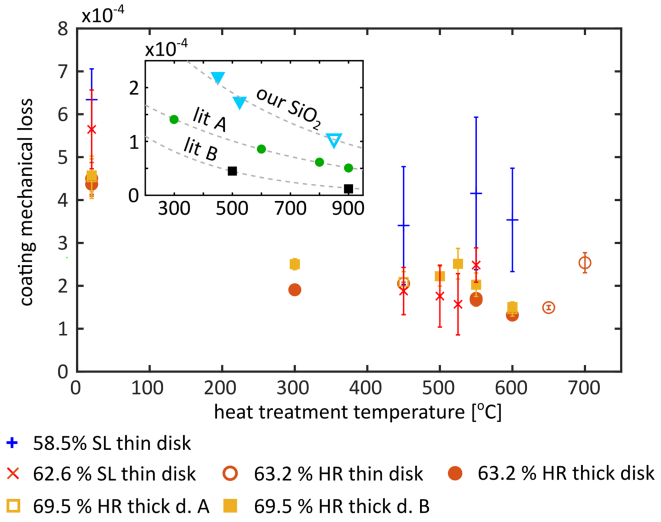

FIG. 1. Mechanical loss of the 58.5% and 62.6% single layers and the HR coatings as a function of heat treatment temperature. Each point represents the average loss of six–eight modes, with the standard deviation used as the error bars. Inset: mechanical loss of our SiO_2 estimated by comparing the single layers and HR losses [33], and SiO_2 loss from the literature *A* [34] and *B* [18]. Axis labels are identical to the main plot.

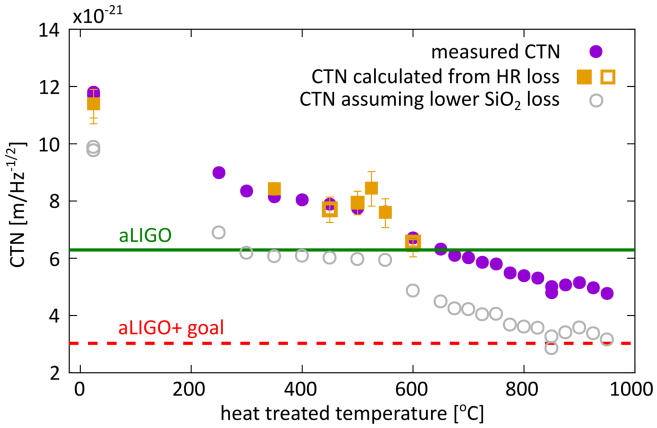

FIG. 2. Directly measured CTN at 100 Hz of the 69.5% HR coating, scaled to the aLIGO end test mass beam size (purple, solid points), and CTN calculated from the HR coating mechanical loss shown by yellow squares, corresponding to the losses in Fig. 1. The gray circles show CTN calculated from individual TiO_2:SiO_2 and SiO_2 losses—see Fig. 1. The red, dashed line represents a reduction compared to aLIGO (green line), which is the CTN goal for the aLIGO + upgrade.

and after coating deposition allows the loss of the coating material to be calculated, using the ratio of the strain energies stored in the coating and substrate found using finite element analysis COMSOL [31]. The coating density, ρ, used in this analysis was found by combining the areal density of the scattering atoms measured by RBS with the measured thickness of the coatings. Resonant modes between 2 kHz and 31 kHz were measured.

Figure 1 shows the average mechanical loss, across six–eight modes, of the 58.5% and 62.3% single layer coatings, and of the two HR stacks. These coatings were deposited on two silica disk geometries: $\text{ø} = 50.8\ \text{mm} \times 1\ \text{mm}$, and $\text{ø} = 76.2\ \text{mm} \times 2.5\ \text{mm}$ (respectively referred to as "thin disk" and as "thick disk" in Fig. 1) [32], heat treated to 950 °C for 4.5 h predeposition. The higher Ti-concentration HR coating was deposited on two different thick disks, labeled *A* and *B*. The coated disks were heat treated, increasing the oven temperature at 100 °C/h to the desired temperature, which was then maintained for 10 h, after which the oven cooled naturally. Following each heat treatment, the mechanical loss was measured.

The mechanical loss of all coatings reduced after their initial heat treatment step (300 °C for the HR stacks, 450 °C for the single layers). The single layer coatings then increased in loss after heat treatment at 550 °C. The HR coatings behaved differently: the loss of the 63.2% HR coating minimizes at 600 °C before starting to increase again, while the 69.5% coating shows a slight increase in loss around 500 °C–550 °C before the loss decreases again at 600 °C. Some mechanical loss HR samples started showing considerable damage such as blisters, cracks, or both, visible by eye after the highest temperature heat treatments.

Interestingly, the single layer and HR coatings with ≈63% Ti concentration have very similar losses, while a lower HR loss would be expected due to the loss of SiO_2 generally being low—see literature data in Fig. 1 (inset) [18,34]. By decomposing our measured HR losses, using the measured TiO_2:SiO_2 single layer losses [35] at 450 °C and 525 °C, we estimated the loss our SiO_2 layers would need to have for the single layer and HR loss to be consistent—this is shown by solid blue triangles in Fig. 1 (inset). The hollow blue triangle assumes further improvement of our SiO_2 with heat treatment at 850 °C, by the same factor (×1.85) as observed for the literature data (green and black points). The gray, dashed lines show exponential least-square fits through all three datasets, indicating their trends. This may suggest that the loss of our SiO_2 is high compared to other SiO_2 films.

Discrepancies of CTN calculated from single layer and HR losses have been observed previously. In the literature no strong evidence of significant interface losses between layers has been found [35,36]. While stress relaxation may cause excess loss particularly on thin substrates [36], it seems unlikely to be the dominant source in our case of relatively thick samples, with consistent loss for different thicknesses. Discrepancies in the literature predominantly arose from differences in the frequency dependence of single-layer and multilayer losses [12,16], which we do not observe. The possibility that SiO_2 is the source of excess loss was concluded before [12,16], although the exact reasons, or if this is the case for our coating, remain unclear.

Coating thermal noise.—CTN was measured directly in a high-finesse cavity (see Gras and Evans for details [37]) using superpolished fused silica substrates of which an 8 mm diameter area in the center was coated with the 69.5%

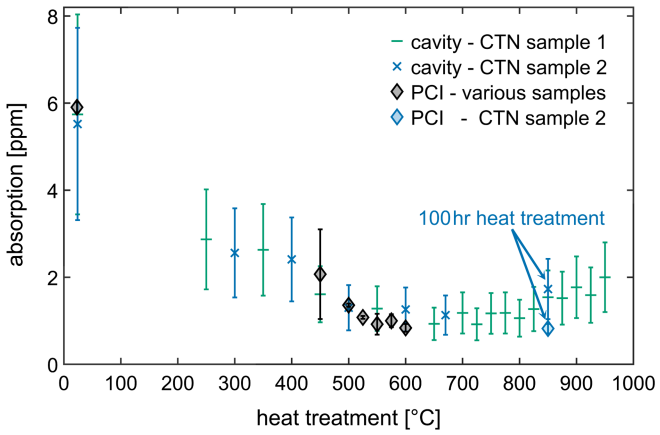

FIG. 3. Optical absorption at 1064 nm of the 69.5% HR stack as a function of heat treatment temperature. The measurement of sample 2 after heat treatment at 850 °C for 100 h is indicated with arrows. All other measurements on both systems were from samples heat treated for 10 h.

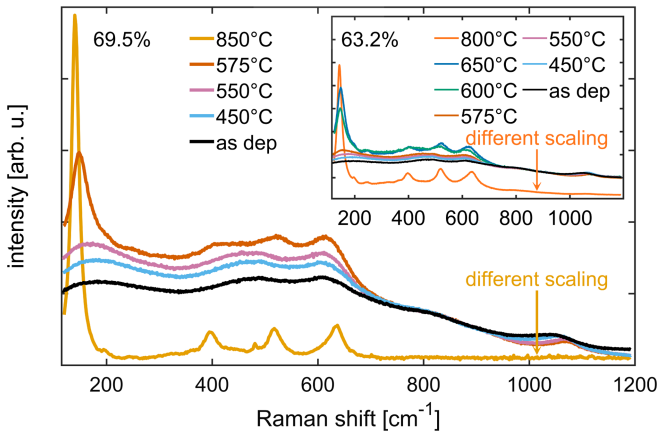

FIG. 4. Raman spectra of the 69.5% HR coating (main plot), and for the 63.2% (inset—axis range identical to main plot). Peak magnitude increases with heat treatment temperature. The data for the 69.5% 850 °C and 63.2% 800 °C heat treated coatings are scaled down with respect to the other spectra.

HR stack. The purple dots in Fig. 2 show the measured CTN at 100 Hz, scaled using Eq. (4) in [37] to the magnitude expected in an aLIGO end test mass mirror (i.e., using a TEM00 mode and a laser beam radius of 6.2 cm). The CTN of our $TiO_2:SiO_2$-based HR stack decreases with increasing heat treatment temperature, reaching the aLIGO CTN level, measured and scaled in the same way (green line), at 650 °C. It then further decreases to a minimum value at 850 °C where it is at 79% of the aLIGO level after 10 h of heat treatment and at 76% after 100 h. Higher temperatures do not show further improvement. Here the oven temperature was increased and decreased by 50 °C/hr, which is a lower rate than used for the mechanical loss samples and notably implemented controlled cooling. None of the CTN samples heat treated in this way developed any cracks or defects below 950 °C. The yellow squares show CTN calculated from the measured mechanical loss of the 69.5% HR coating (yellow squares in Fig. 1), agreeing within $\lesssim 4\%$ of the directly measured CTN.

To estimate the effect of potentially high SiO_2 loss, or other excess loss in the stack, the fit through the blue triangles (Fig. 1, inset) was used to extract the $TiO_2:SiO_2$ loss from the directly measured CTN at each temperature. The result was combined with the best SiO_2 loss from the literature (black squares in Fig. 1) [38] to calculate the CTN shown by the gray circles in Fig. 2. This analysis suggests that a maximum CTN reduction to ≈45% of aLIGO/AdV could be achieved, beating the aLIGO + goal of 50% CTN reduction, if the excess loss was reduced. If the SiO_2 itself is the excess loss source, improved SiO_2 could also possibly reduce the loss of the $TiO_2:SiO_2$ layers in the coating, further improving performance.

Optical absorption.—The optical absorption of the 69.5% $TiO_2:SiO_2$ HR coating used for direct CTN measurements was determined by measuring the resonant frequency of the high-finesse cavity as a function of circulating power. Heating from the absorbed power changes the optical path length in the cavity via thermal expansion and dn/dT, resulting in a change in resonant frequency that is proportional to the circulating power. A sample of known absorption is used to calibrate the measurement. Each measurement was made using a single 50 μm laser-beam spot near the center of the coating surface, resulting in absorption values shown as green dashes and blue crosses in Fig. 3. The absorption reduces with increasing heat treatment temperature to a minimum of (0.9 ± 0.4) ppm at 650 °C, and then remains fairly constant until it starts to slightly increase at 800 °C.

The absorption was also measured using photothermal common-path interferometry (PCI) [39], a technique to measure very low optical absorption with a high spatial resolution. For these measurements, the mechanical loss disks were used as well as some smaller-scale samples coated in the same coating run. Samples heat treated for 10 h at target temperatures up to 600 °C were measured, shown as black diamonds in Fig. 3, where the optical absorption reduced to (0.84 ± 0.09) ppm. The sample used for direct CTN measurements, heat treated to 850 °C for 100 h, was also measured with PCI, shown as a blue diamond, yielding absorption of (0.82 ± 0.10) ppm.

Crystallization and defects.—Raman spectroscopy on the 69.5% HR coating was carried out to assess crystallization after heat treatment. The as-deposited coating, and the lower temperature heat treatments, show a characteristic amorphous spectrum with broad Raman bands, see Fig. 4, consistent with being a combination of SiO_2 and TiO_2. The coating starts crystallizing (as anatase) between 550 °C and 575 °C, as evidenced by the narrower peaks in the spectrum, which is a significantly higher temperature than for

pure IBS-TiO_2 [40,41]. Through heat treatment, the peaks converge on bulk crystalline anatase TiO_2 values [42] in all cases except the primary peak where a progressive red shift is seen—settling at 140 cm^{-1} after 850 °C. This shift may result from stresses arising from the thermal mismatch of the materials [43], and its position is only clearly resolved after advanced crystallization. It could also originate from increasing oxygen content in the high-n layers as a result of heat treatment in air [44,45] or potential interdiffusion from neighboring SiO_2 layers [46]. The inset shows the results for the 63.2% HR coating, which starts crystallizing at 600 °C, doing so as both anatase and rutile.

Macroscopic defects were noted for many of the mechanical loss samples at higher heat treatment temperatures: HR stacks of both compositions on three different 76.2 mm disks started showing blisters, mainly in a ring-shape near the edge, after heat treatment at 600 °C, while the 63.2% HR coating on a 50.8 mm disk did not show blisters, but started cracking after heat treatment at 650 °C. It is interesting to note that the 76.2 mm disks were polished to a better surface quality, i.e., lower rms surface roughness, than the 50.8 mm disk.

The samples used for direct CTN measurements did not show any blistering, while cracks were only observed after heat treatment at 950 °C. Possible reasons could be (i) that the coatings were of a smaller diameter, (ii) that the coating ended several millimeters away from the substrate edges while the other samples were completely coated, or (iii) that a controlled cool-down rate after heat treatment was used, which was much slower than the natural cool-down rate used for the other samples.

Scattering.—total integrated scatter (TIS) of the 69.5% HR coating was measured using two techniques. The first used an integrating sphere, which has a scattered light capture range from 1 to 75° [47], and a 0.3 mm diameter 1064 nm laser beam, while the second used an angle-resolved scatterometer (ARS) which records the scattered light at discrete angles between 3 and 80°, using a 5.2 mm diameter 1056 nm beam from a superluminescent diode. With the ARS, integrated scatter over this range of angles is estimated assuming isotropic scattering in azimuthal angles [48].

For the as-deposited HR stack, the integrating sphere measurement gave a TIS of (2.8 ± 1.0) ppm and the ARS yielded (2.9 ± 1.0) ppm. For the HR stack heat treated at 850 °C for 100 h, the TIS was higher, but still at a relatively low level: (4.6 ± 1.0) ppm from the integrating sphere and (5.2 ± 1.9) ppm from the ARS. In comparison, the TIS of the aLIGO mirror coatings have been measured to be (9.5 ± 2.0) ppm [47] using the same integrating sphere setup, while another technique [49] yielded a value of (4.9 ± 1.5) ppm [13]. While care is needed when comparing our test sample to the aLIGO mirrors, due to the difference in size of the coating and differences in the substrate surface quality, these initial scatter results for the optimally heat-treated, defect-free and partially crystallized $TiO_2:SiO_2$ HR coating are very promising.

Discussion.—We have shown by direct CTN measurements that HR coatings made of 69.5% $TiO_2:SiO_2$ and SiO_2 have the potential to reduce CTN to 76% of the aLIGO CTN. From comparing the measured losses of the $TiO_2:SiO_2$ single layer and HR coatings, we conclude that either the SiO_2 in our coatings has a much higher loss than expected based on the literature data, or some other excess loss is present. When combining our $TiO_2:SiO_2$ with the loss of state-of-the-art SiO_2, we calculate a lower boundary of 45% of aLIGO/AdV CTN. Therefore, further investigation of the reason for the discrepancy between single layer and HR loss is of high interest. While the TiO_2 in our 69.5% HR coating begins to crystallize at 575 °C, with crystallization resulting in a scattering increase of about a factor of 2 at 850 °C, it is very interesting to note that the resulting scattering level is still comparable to, or better than, that of an aLIGO coating. While some coating samples displayed a small number of defects at higher heat treatment temperatures, other samples survived with no defects until a temperature of 950 °C was reached, demonstrating that this material has the potential to survive the annealing temperatures required for optimum CTN performance. After heat treatment at 850 °C for 100 h, the HR coating had an absorption of (0.82 ± 0.10) ppm.

Overall, this coating has high potential for providing improved CTN, compared to aLIGO and AdV, in room-temperature gravitational-wave detectors while also showing promising optical properties.

We are grateful for financial support from STFC (ST/V005634/1, ST/V001736/1), the University of Glasgow, the Royal Society (RG110331), ETpathfinder (Interreg Vlaanderen-Nederland), E-TEST (Interreg Euregio Meuse-Rhine), the Province of Limburg and National Science Foundation Awards No. PHY-2207998 and No. PHY-2219109. Work done at U. Montréal is funded by NSERC, CFI, and FRQNT through the RQMP. We thank our colleagues within the LIGO Scientific Collaboration and Virgo Collaboration and within SUPA for their interest in this work. This Letter has LIGO Document No. P2300203. LIGO was constructed by the California Institute of Technology and Massachusetts Institute of Technology with funding from the National Science Foundation, and operates under cooperative agreement PHY-1764464.

G. I. M., V. S., and N. D. contributed equally to this work.

*Jessica.Steinlechner@ligo.org

[1] A. Einstein, *Näherungsweise Integration der Feldgleichungen der Gravitation* (Springer Berlin Heidelberg, Berlin, Heidelberg, 2018), pp. 149–158, 10.1007/978-3-662-57411-9_13.

[2] A. Einstein, *Über Gravitationswellen* (John Wiley & Sons, Ltd, New York, 2005), pp. 135–149, https://onlinelibrary.wiley.com/doi/abs/10.1002/3527608958.ch12.

[3] B. P. Abbott, R. Abbott, T. D. Abbott, M. R. Abernathy, F. Acernese, K. Ackley, C. Adams, T. Adams, P. Addesso, R. X. Adhikari *et al.*, Observation of Gravitational Waves from a Binary Black Hole Merger, Phys. Rev. Lett. **116**, 061102 (2016).

[4] B. P. Abbott, R. Abbott, T. D. Abbott, F. Acernese, K. Ackley, C. Adams, T. Adams, P. Addesso, R. X. Adhikari, V. B. Adya *et al.*, GW170817: Observation of Gravitational Waves from a Binary Neutron Star Inspiral, Phys. Rev. Lett. **119**, 161101 (2017).

[5] R. Abbott, T. D. Abbott, S. Abraham, F. Acernese, K. Ackley, A. Adams, C. Adams, R. X. Adhikari, V. B. Adya, C. Affeldt *et al.*, GWTC-2: Compact Binary Coalescences Observed by LIGO and Virgo During the First Half of the Third Observing Run, Phys. Rev. X **11**, 021053 (2021).

[6] R. Abbott, T. D. Abbott, F. Acernese, K. Ackley, C. Adams, N. Adhikari, R. X. Adhikari, V. B. Adya, C. Affeldt *et al.*, GWTC-3: Compact binary coalescences observed by LIGO and Virgo during the second part of the third observing run, arXiv:2111.03606v2.

[7] B. P. Abbott, R. Abbott, T. D. Abbott, M. R. Abernathy, F. Acernese, K. Ackley, C. Adams, T. Adams, P. Addesso, R. X. Adhikari *et al.*, GW150914: The Advanced LIGO Detectors in the Era of First Discoveries, Phys. Rev. Lett. **116**, 131103 (2016).

[8] F. Acernese *et al.*, Advanced Virgo: A second-generation interferometric gravitational wave detector, Classical Quantum Gravity **32**, 024001 (2015).

[9] W. Yam, S. Gras, and M. Evans, Multimaterial coatings with reduced thermal noise, Phys. Rev. D **91**, 042002 (2015).

[10] T. Hong, H. Yang, E. K. Gustafson, R. X. Adhikari, and Y. Chen, Brownian thermal noise in multilayer coated mirrors, Phys. Rev. D **87**, 082001 (2013).

[11] Laboratoire des Matériaux Avancés, https://lma.in2p3.fr.

[12] M. Granata, A. Amato, L. Balzarini, M. Canepa, J. Degallaix, D. Forest, V. Dolique, L. Mereni, C. Michel, L. Pinard, B. Sassolas, J. Teillon, and G. Cagnoli, Amorphous optical coatings of present gravitational-wave interferometers, Classical Quantum Gravity **37**, 095004 (2020).

[13] L. Pinard *et al.*, Mirrors used in the LIGO interferometers for first detection of gravitational waves, Appl. Opt. **56**, C11 (2017).

[14] G. Harry *et al.*, Thermal noise from optical coatings in gravitational wave detectors, Appl. Opt. **45**, 1569 (2006).

[15] G. M. Harry, M. R. Abernathy, A. E. Becerra-Toledo, H. Armandula, E. Black, K. Dooley, M. Eichenfield, C. Nwabugwu, A. Villar, D. R. M. Crooks, G. Cagnoli, J. Hough, C. R. How, I. MacLaren, P. Murray, S. Reid, S. Rowan, P. H. Sneddon, M. M. Fejer, R. Route, S. D. Penn, P. Ganau, J.-M. Mackowski, C. Michel, L. Pinard, and A. Remillieux, Titania-doped tantala/silica coatings for gravitational-wave detection, Classical Quantum Gravity **24**, 405 (2006).

[16] A. Amato, G. Cagnoli, M. Granata, B. Sassolas, J. Degallaix, D. Forest, C. Michel, L. Pinard, N. Demos, S. Gras, M. Evans, A. Di Michele, and M. Canepa, Optical and mechanical properties of ion-beam-sputtered Nb_2O_5 and $TiO_2 - Nb_2O_5$ thin films for gravitational-wave interferometers and an improved measurement of coating thermal noise in Advanced LIGO, Phys. Rev. D **103**, 072001 (2021).

[17] M. A. Fazio, G. Vajente, L. Yang, A. Ananyeva, and C. S. Menoni, Comprehensive study of amorphous metal oxide and Ta_2O_5-based mixed oxide coatings for gravitational-wave detectors, Phys. Rev. D **105**, 102008 (2022).

[18] M. Granata *et al.*, Progress in the measurement and reduction of thermal noise in optical coatings for gravitational-wave detectors, Appl. Opt. **59**, A229 (2020).

[19] G. Vajente *et al.*, Low Mechanical Loss $TiO_2:GeO_2$ Coatings for Reduced Thermal Noise in Gravitational Wave Interferometers, Phys. Rev. Lett. **127**, 071101 (2021).

[20] A. Davenport *et al.*, The development of high reflection $TiO_2:GeO_2$ and SiO_2 coatings for gravitational wave detectors, in *Proceedings of the Optical Interference Coatings Conference (OIC) 2022* (Optica Publishing Group, 2022), p. WA.6, https://opg.optica.org/abstract.cfm?URI=OIC-2022-WA.6.

[21] C. S. Menoni, L. Yang, M. Fazio, G. Vajente, A. Ananyeva, G. Billingsley, F. Schiettekatte, M. Chicoine, A. Markosyan, R. Bassiri, and M. M. Fejer, Survey of metal oxides for coatings of ultra-stable optical cavities, in *Proceedings of the 2021 Conference on Lasers and Electro-Optics (CLEO)* (2021), pp. 1–2, https://opg.optica.org/abstract.cfm?URI=CLEO_SI-2021-STu1C.7.

[22] S. Chao, W.-H. Wang, and C.-C. Lee, Low-loss dielectric mirror with ion-beam-sputtered TiO_2–SiO_2 mixed films, Appl. Opt. **40**, 2177 (2001).

[23] FiveNine Optics, https://www.fivenineoptics.com/.

[24] W.-K. Chu, J. W. Mayer, and M.-A. Nicolet, *Backscattering Spectrometry* (Academic Press, New York, 1978), https://www.sciencedirect.com/science/article/pii/B9780121738501500028.

[25] M. Mayer, SIMNRA, a simulation program for the analysis of NRA, RBS and ERDA, AIP Conf. Proc. **475**, 541 (1999).

[26] M. Chicoine, F. Schiettekatte, M. Laitinen, and T. Sajavaara, Oxy-nitrides characterization with a new ERD-TOF system, Nucl. Instrum. Methods Phys. Res., Sect. B **406**, 112 (2017).

[27] WTheiss Hardware and Software, http://www.wtheiss.com/.

[28] O. S. Heavens, *Thin Film Physics* (Methuen, 1970), Vol. 95.

[29] J. Steinlechner, Development of mirror coatings for gravitational-wave detectors, Phil. Trans. R. Soc. A **376**, 20170282 (2018).

[30] E. Cesarini, M. Lorenzini, E. Campagna, F. Martelli, F. Piergiovanni, F. Vetrano, G. Losurdo, and G. Cagnoli, A "gentle" nodal suspension for measurements of the acoustic attenuation in materials, Rev. Sci. Instrum. **80**, 053904 (2009).

[31] COMSOL, COMSOL Multiphysics User's Guide, The Heat Transfer Branch (2012), pp. 709–745, https://doc.comsol.com/5.5/doc/com.comsol.help.comsol/COMSOL_ReferenceManual.pdf.

[32] A set of "thick disk" single layers was also coated and heat treated to 300 °C, however, the thickness ratio of coatings and substrates was too small ($\lessapprox 10^{-4}$) for the coating loss to be extracted from those samples.

[33] D. R. M. Crooks, Mechanical loss and its significance in the test mass mirrors of gravitational wave detectors, Ph.D. thesis, University of Glasgow, 2002, http://theses.gla.ac.uk/id/eprint/2893.

[34] R. Robie, Characterisation of the mechanical properties of thin-film mirror coating materials for use in future interferometric gravitational wave detectors, Ph.D. thesis, University of Glasgow, 2018, http://theses.gla.ac.uk/id/eprint/30645.

[35] S. D. Penn, P. H. Sneddon, H. Armandula, J. C. Betzwieser, G. Cagnoli, J. Camp, D. R. M. Crooks, M. M. Fejer, A. M. Gretarsson, G. M. Harry, J. Hough, S. E. Kittelberger, M. J. Mortonson, R. Route, S. Rowan, and C. C. Vassiliou, Mechanical loss in tantala/silica dielectric mirror coatings, Classical Quantum Gravity **20**, 2917 (2003).

[36] M. Granata, E. Saracco, N. Morgado, A. Cajgfinger, G. Cagnoli, J. Degallaix, V. Dolique, D. Forest, J. Franc, C. Michel, L. Pinard, and R. Flaminio, Mechanical loss in state-of-the-art amorphous optical coatings, Phys. Rev. D **93**, 012007 (2016).

[37] S. Gras and M. Evans, Direct measurement of coating thermal noise in optical resonators, Phys. Rev. D **98**, 122001 (2018).

[38] Other parameters used for SiO_2 were $n = 1.45$, a Young's modulus of 73.2 GPa and a Poisson ratio of 0.11, which are parameters identical to those of Granata, used by Vajente [18,19].

[39] A. Alexandrovski, M. Fejer, A. Markosian, and R. Route, Photothermal common-path interferometry (PCI): New developments, Solid State Lasers XVIII **7193**, 71930D (2009).

[40] C. She, Raman characterization of optical thin film coatings, Thin Solid Films **154**, 239 (1987).

[41] C.-C. Lee and C.-J. Tang, TiO_2–Ta_2O_5 composite thin films deposited by radio frequency ion-beam sputtering, Appl. Opt. **45**, 9125 (2006).

[42] L. Kernazhitsky, V. Shymanovska, T. Gavrilko, V. Naumov, L. Fedorenko, V. Kshnyakin, and J. Baran, Laser-excited excitonic luminescence of nanocrystalline TiO_2 powder, Ukr. J. Phys. **59**, 246 (2014).

[43] D. Liu and P. Flewitt, *Raman Measurements of Stress in Films and Coatings* (2014), Vol. 45, pp. 141–177, 10.1039/9781782621485-00141.

[44] J. C. Parker and R. W. Siegel, Raman microprobe study of nanophase TiO_2 and oxidation-induced spectral changes, J. Mater. Res. **5**, 1246 (1990).

[45] J. C. Parker and R. W. Siegel, Calibration of the Raman spectrum to the oxygen stoichiometry of nanophase TiO_2, Appl. Phys. Lett. **57**, 943 (1990).

[46] A. Krost, W. Richter, D. R. T. Zahn, K. Hingerl, and H. Sitter, Chemical reaction at the ZnSe/GaAs interface detected by Raman spectroscopy, Appl. Phys. Lett. **57**, 1981 (1990).

[47] G. Billingsley, H. Yamamoto, and L. Zhang, Characterization of Advanced LIGO core optics, Vol. 66 American Society for Precision Engineering (ASPE) (2017), pp. 78–83, https://www.proceedings.com/37625.html.

[48] F. Magana-Sandoval, R. X. Adhikari, V. Frolov, J. Harms, J. Lee, S. Sankar, P. R. Saulson, and J. R. Smith, Large-angle scattered light measurements for quantum-noise filter cavity design studies, J. Opt. Soc. Am. A **29**, 1722 (2012).

[49] J. Degallaix, C. Michel, B. Sassolas, A. Allocca, G. Cagnoli, L. Balzarini, V. Dolique, R. Flaminio, D. Forest, M. Granata, B. Lagrange, N. Straniero, J. Teillon, and L. Pinard, Large and extremely low loss: The unique challenges of gravitational wave mirrors, J. Opt. Soc. Am. A **36**, C85 (2019).